Supporting Information

# 5-Aminolevulinic Acid Loaded Ethosomal Vesicles with High Entrapment Efficiency for *in Vitro* Topical Transdermal Delivery and Photodynamic Therapy of Hypertrophic Scars

Zheng Zhang[a,†], Yunsheng Chen[b,†], Heng Xu[a,†], Yan Wo[c], Zhen Zhang[d], Ying Liu[e], Weijie Su[a,*], Daxiang Cui[b,*] and Yixin Zhang[a,*]

[a] Department of Plastic and Reconstructive Surgery, Shanghai Ninth People's Hospital, School of Medicine, Shanghai Jiao Tong University, 639 Zhizaoju Rd, Shanghai 200011, P.R. China;

[b] Institute of Nano Biomedicine and Engineering, Shanghai Engineering Research Center for Intelligent Instrument for Diagnosis and Therapy, School of Biomedicine Engineering, 800 Dongchuan Rd, Shanghai Jiao Tong University, Shanghai 200240, P.R. China;

[c] Department of Human Anatomy, Histology and Embryology, School of Medicine, Shanghai Jiao Tong University, 227 South Chongqing Rd, Shanghai 200025, P.R. China;

[d] Department of Dermatology, Shanghai Ninth People's Hospital, School of Medicine, Shanghai Jiao Tong University, 639 Zhizaoju Rd, Shanghai 200011, P.R. China.

[e] Cosmetic Laser Center, Shanghai Ninth People's Hospital, School of Medicine, Shanghai Jiao Tong University, 639 Zhizaoju Rd, Shanghai 200011, P.R. China

† These authors contributed equally to this work.

* Authors to whom correspondence should be addressed; E-Mail: rosiewudi@163.com; dxcui@sjtu.edu.cn; zhangyixin6688@163.com

## S1. Figure captions

**Figure S1** The chemical structure of 5-aminolevulinic acid (ALA)

**Figure S2** The size distribution of prepared ALE-ES.

**Figure S3** The transmission electron microscopy (TEM) images of ALA-ES with different irregular appearances when penetrating into hypertrophic scars.

**Figure S4**. The fluorescence spectra of ALA with different concentrations (a to f: 0.1, 1, 5, 10, 20 and 50 μg/ml). Insert: calibration curve for ALA in citrate buffer solution (CBS).

**Figure S5** The influence factors of EE in preparing ALA-ES by pH gradient active loading method. (A) transmembrane pH gradient, (B) incubation conditions, (C) ALA-ES size and (D) PC concentration

**S2 The calculation of entrapment efficiency (EE)**

ALA was rapidly and accurately detected by a modified fluoresceamine derivatization approach using 96-well micro-plates, and the details were shown in **S3, Supplementary Material**. ALA-ES were separated from the untrapped ALA by an ultrafiltration-centrifugation method using Amicon® Ultra-0.5 filters (molecular weight cut-off (MWCF) 30 KDa, Millipore, USA). Considering the non-specific adsorption between free ALA and filters, it was necessary to determine the recovery (R') by ultrafiltration of 200 μL ALA standard solution (5, 20, 100 μg/mL ALA in PBS, 0.01 M, pH 7.4). The R' was calculated by the following equation (1), where the $m_t$ was the total mass of ALA before ultrafiltration and mf was the mass of ALA in the ultrafiltrate.

$$R' = m_f / m_t \times 100\% \quad (1)$$

For EE determination, 20 μL ALA-ES suspension was diluted to 200 μL with PBS, and then placed in an Amicon® Ultra-0.5 filters (MWCF 30 KDa, Millipore, USA). The sample was centrifuged at the speed of 5000 rpm for 30 min to separate the untrapped ALA from ALA-ES. Then the ultrafiltrates were carefully collected and diluted to 1 mL with PBS, and the ALA amount in ultrafiltrate ($Q_f$) and total ALA amount added ($Q_t$) were determined, respectively. Then EE equation was adjusted as follows:

$$EE = (1 - Q_f / (R' \times Q_t)) \times 100\%. \quad (2)$$

**S3 Quantitative analytical of ALA using 96-well microplate**

A modification of fluorescamine derivatization procedure was used to quantitative detection of ALA. Briefly, 12 μL sample, 270 μL fluorescamine dissolved in acetonitrile (0.1%, w/v), 45 μL borate buffer solution (BBS, 0.1 M, pH 8.0), and 570 μl water were added into a microfuge tube in sequence. The mixture was vortexed for 5 s and allowed to react in dark environment for 5 min. The fluorescence spectra (excitation and emission wavelength) were recorded with a Hitachi FL-4600 spectrofluorometer (Tokyo, Japan). For EE measurement, 300 μL reacted mixtures were transferred to the wells of a flat-bottomed microplate (96 well, Corning, USA) and their fluorescence intensities were obtained by a Synergy H4 hybrid reader (Bio-Tek, USA) with 380 nm excitation/ 480 nm emission. Each sample was set three replicates and the average fluorescence intensity was calculated. In addition, blank samples consisting of PBS (to substitute for ALA), BBS, and fluorescamine dissolved in acetonitrile were prepared and used to correct for background fluorescence.

Figure S4 showed the fluorescence spectra of ALA in CBS with a concentration range from 0.5 to 50 μg/mL. It could be observed that the relative fluorescence intensity (RFI) at 480 nm presented a good linearity with ALA concentration (C), and the regression equation was $RFI = 301.5*C+183.56$, with a correlation coefficient (r) of 0.9996. In order to preclude the inconformity of fitting equations from different microplates, we set up a blank control and standard solutions of ALA on every microplate, and the *r* value of each fitting equation was more than 0.999, meaning the *RFI* was significantly correlated with ALA concentration from 0.5 to 50 μg/mL. In addition, 2% (*w/v*) PC solution, 30% (*v/v*) hydroalcoholic solution and non-drug-loading ES solution were reacted with fluorescamine, respectively, and no detectable fluorescence emission peak was found from 400 nm to 600 nm (λex = 380 nm), indicating these ingredients wouldn't interfere with the derivatization procedure.

## S4 Optimization of preparing ALA-ES

To obtain a favorable EE of ALA-ES, several effect factors in preparation of ALA-ES, including transmembrane pH gradient, incubation conditions, ALA-ES size and PC concentration were optimized as follows.

### S4.1 Effect of transmembrane pH gradient

ALA, as a zwitterion, possesses two ionization sites ($pK_a$ 4.0 and $pK_b$ 8.20). It keeps stable in acidic solutions (pH $\leq$ 5.5), and tends to dimerize under alkaline conditions.[1] However, the PC hydrolysis would exacerbate in acidic solution with pH $\leq$ 3.0.[2] Therefore, pH 4.0 of internal phase was chosen. The external phase was adjusted to different pH values (5.0, 6.0, 7.0, 7.4, and 8.0). The result was shown in Figure S5A. When external pH was lower than 7.0, EE was around 10.0% with no significant difference from pH 5.0 and 6.0 ($P > 0.05$). With increasing the external pH from 7.0 to 8.0, the EE of ALA-ES increased from 10.0 % to 44.5% ($P < 0.05$), but there was no significant difference of EE between external pH 7.4 and 8.0 ($P > 0.05$). The results showed that pH gradient across vesicular membrane served as an efficient driving force to load and accumulate ALA inside ES vesicles. With transmembrane pH gradient increased, more and more ALA was loaded into ES vesicles until internal proton pool was depleted and the EE would not increase any more.[3] Considering the skin irritation of ALA-ES system with external pH 8.0, the optimum external phase pH was fixed as 7.4.

### S4.2 Effect of incubation conditions

A proper incubation temperature was necessary to conquer the ES membrane permeability barrier (activation energy) and help ALA loading. Different incubation temperatures (30, 40 and 60 $^{o}$C) with different incubation time (0.25, 0.5, 1.0, 1.5, 2.0, 2.5, 3.0 and 4.0 h) were examined in this part. In

Figure S5B, when the incubation was performed at 30 °C, it would take 2.5 h to reach the maximum EE of 35%. When the incubation was performed at 40 °C, it could reach a maximum EE around 48% after 3 h, No obvious drug loading happened when the samples were incubated at 60 °C. These results indicated that maintaining optimal temperature and time in this active loading method were very important for efficient and stable drug loading. Raising the incubation temperature could enhance the permeability of ES and was favour of drug loading. However, high temperature could result in PC hydrolysis and the collapse of the pH gradient, leading to increased leakage of drug from vesicles and compromised drug loading[2, 42, 4]. An incubation period of 3h at 40 °C was proper in this study. With the encapsulation of ALA, the transmembrane pH gradient continued to decrease, and when it can't drive ALA molecules across the bilayer, further prolonging incubation time will no longer increase EE of ALA ES at 40°C.

**S4.3 Effect of ALA-ES size**

To investigate the influence of different particle size on EE, ALA-ES formulations undergoing different sonication time were prepared. As shown in Figure S5C, with increasing sonication time, the EE significantly increased from 15% to 49% ($P < 0.05$), and the average ALA-ES size showed a reverse trend from 220 to 54 nm. The results could be explained as following. During agitation procedure before sonication, the lipid dissolved in the hydroalcoholic suspension self-close to form large multi-lamellar vesicles with small aqueous cores encapsulated by multiple concentric bilayers. Sonication could disrupt multi-lamellar vesicles and rearrange the lipid bilayers to form more amounts of smaller, less lamellar vesicles but with a relatively lager internal cores. This might be the reason why EE of ALA-ES increased with the vesicle size decreased during the sonication. Furthermore, ES with a smaller size was in favor of its penetration into HS, which has been verified in our previous work.[5] Therefore, ES with particle size around 54 nm after 20 min sonication was

selected.

**S4.4 Effect of PC concentration**

Different concentrations of PC (0.5 to 4.0%, w/v) were used to prepare ALA-ES within 50-80 nm in Figure S5D. During the preparation, we found that with the PC concentration raised, increased sonication period was needed to obtain the required vesicular size. For instance, it took 5 min ultrasonic dispersion to obtain 60 nm ALA-ES with 0.5% PC, but more than 40 min ultrasonic dispersion for 80 nm ALA-ES with 4.0% PC. Generally speaking, given the ALA amount (0.2%, w/v), more PC could produce more ES, and then more ALA could be loaded. Therefore, when PC concentration increased from 1.0% to 2.0%, EE of ALA-ES exhibited a significant improvement ($P < 0.05$). However, EE slightly decreased when PC further increased from 3% to 4%. This phenomenon might be due to the lack of stability of ES with high concentration PC in small dimension.[6] In this condition, ES tend to aggregate together and fuse to bigger and inhomogeneous micelles, leading to decreased permeability of surface area, heterogeneous interior liquid phase and pH value, which were great adverse to ALA entrapment. In addition, prolonged sonication might destroy the integrity of ES and lead to the collapse of transmembrane pH gradient. With comprehensive consider-ation of the EE and stability, 2% was the proper PC concentration.

After optimization, the prepared ALA-ES had excellent EE of 50.6% and small size of 54 nm under the selected conditions, which was a great improvement of that of lower than 10% by passive loading method ever reported.

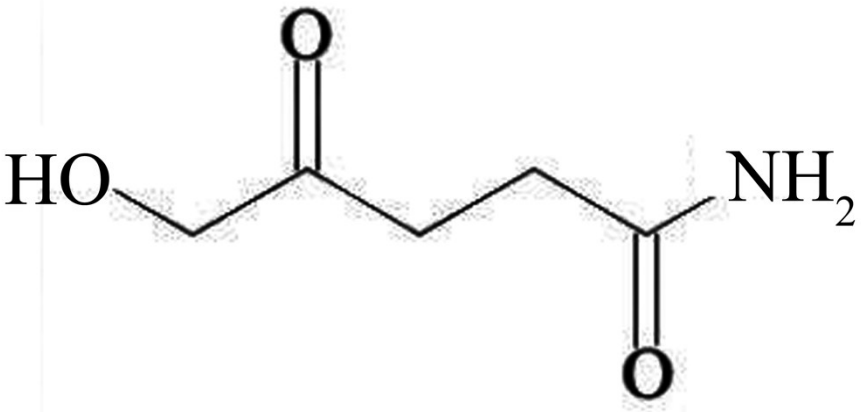


**Figure S1**

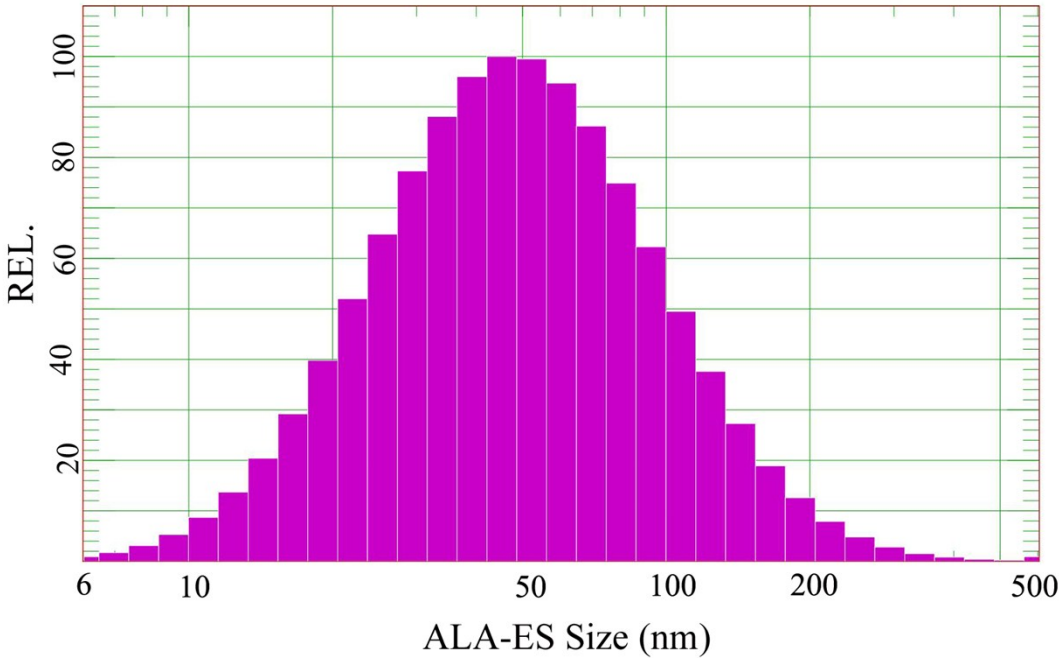


**Figure S2**

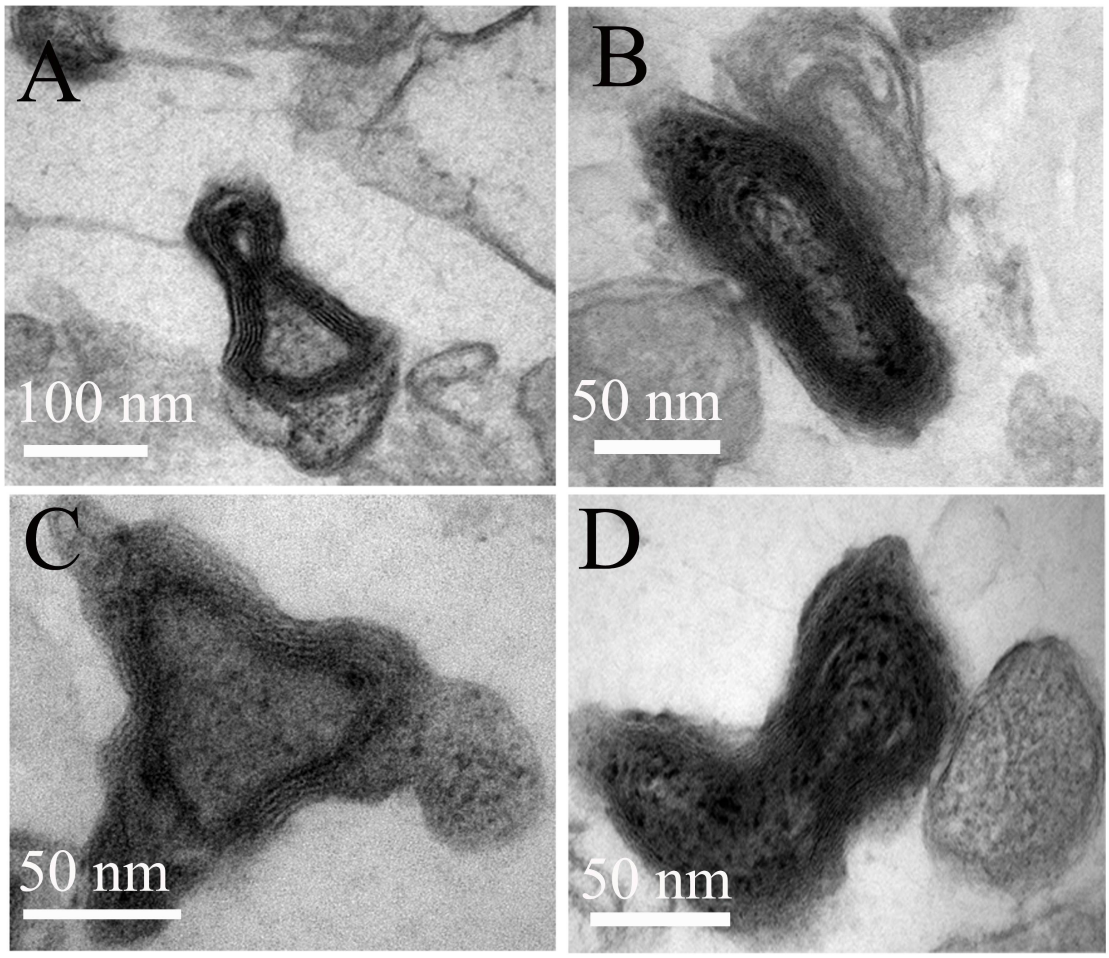


**Figure S3**

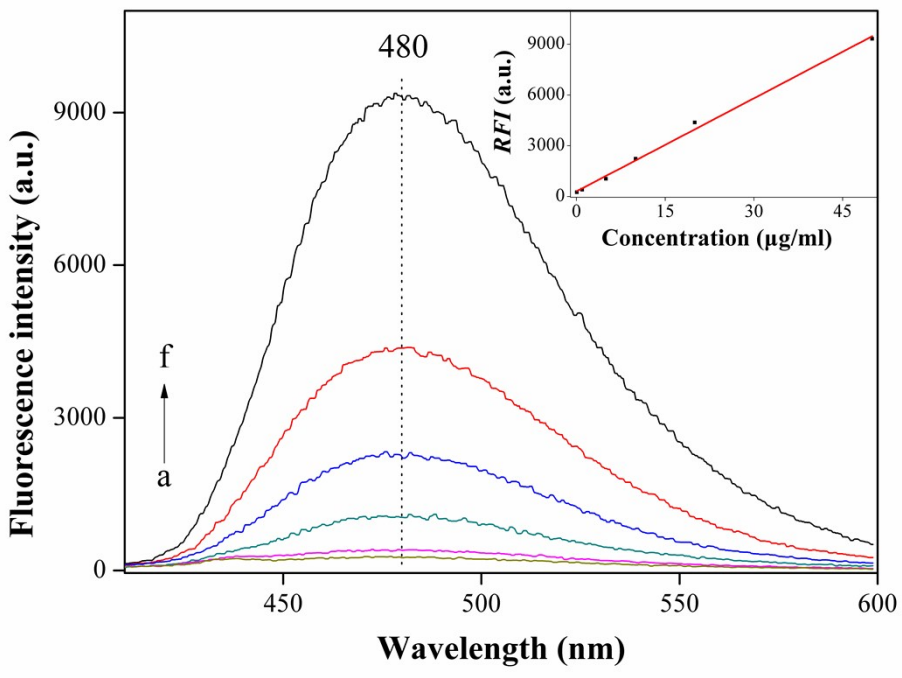
480
9000
6000
3000
0
Fluorescence intensity (a.u.)
f
a
450
500
550
600
Wavelength (nm)
RFI (a.u.)
9000
6000
3000
0
0
15
30
45
Concentration (μg/ml)

**Figure S4**

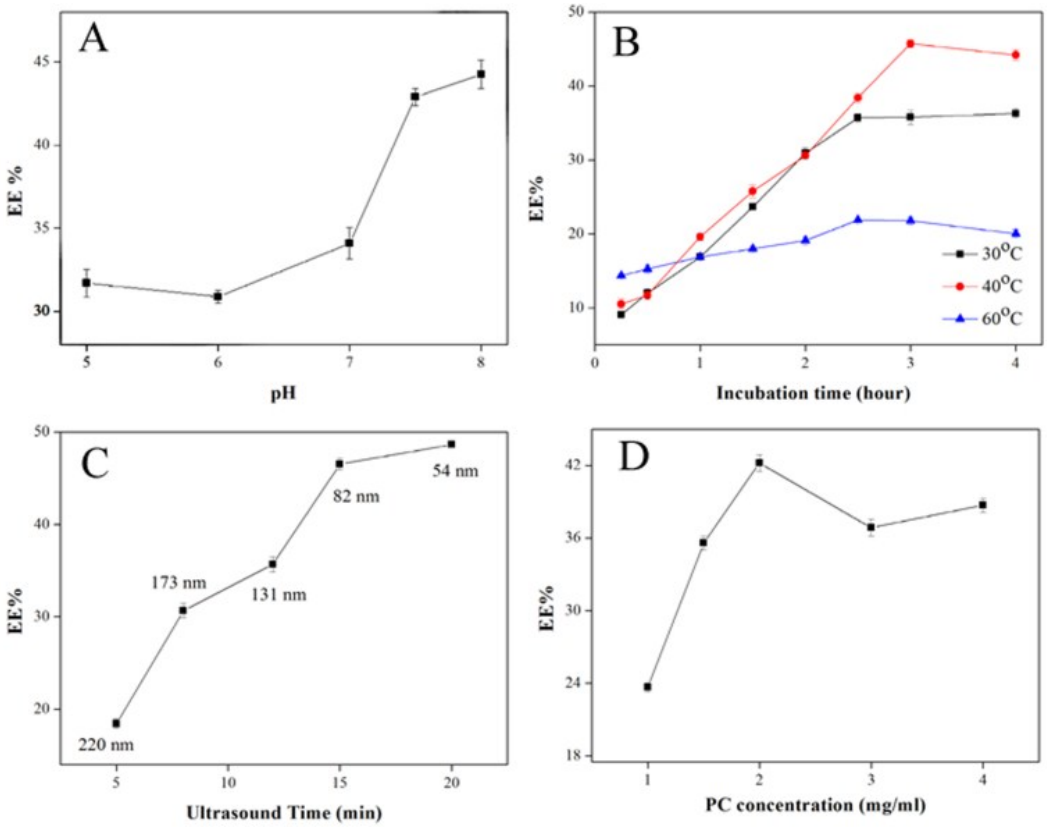
A
EE %
pH
B
EE%
Incubation time (hour)
30°C
40°C
60°C
C
EE%
Ultrasound Time (min)
220 nm
173 nm
131 nm
82 nm
54 nm
D
EE%
PC concentration (mg/ml)

**Figure S5**

**Table S1** the retention and permeation results of both ALA-ES and ALA-HA.

| Time (h) | Retention amount (%) | | Permeation amount (%) | | Total penetration (%) | |
|---|---|---|---|---|---|---|
| | ALA-ES | ALA-HA | ALA-ES | ALA-HA | ALA-ES | ALA-HA |
| 0.25 | 22.91±3.38 | 19.52±2.24 | 15.89±1.31 | 8.74±1.27 | 38.81±2.31 | 28.27±1.72 |
| 0.5 | 56.17±4.47 | 36.73±2.14 | 12.77±2.53 | 11.38±2.37 | 68.94±3.46 | 48.12±2.22 |
| 1.0 | 62.62±3.43 | 46.04±3.34 | 10.51±1.36 | 9.61±1.23 | 73.13±2.39 | 55.65±2.27 |
| 1.5 | 67.74±3.27 | 43.87±5.27 | 14.59±2.64 | 14.90±1.53 | 82.34±2.92 | 58.78±3.36 |
| 2.0 | 80.79±3.18 | 50.36±6.32 | 12.84±3.19 | 8.50±2.84 | 93.64±3.15 | 58.86±4.16 |
| 3.0 | 75.82±4.61 | 55.58±2.39 | 19.69±3.55 | 14.26±3.52 | 95.51±4.05 | 69.84±2.9o |
| 6.0 | 60.89±3.25 | 59.66±3.31 | 37.29±2.32 | 15.22±1.49 | 98.18±2.78 | 74.88±2.35 |
| 12.0 | 28.88±4.43 | 15.31±1.28 | 68.09±5.23 | 60.44±2.75 | 96.98±4.81 | 75.75±1.95 |

## References


1. A. Bunke, O. Zerbe, H. Schmid, G. Burmeister, H. Merkle and B. Gander, *Journal of pharmaceutical sciences*, 2000, **89**, 1335-1341.
2. Y. Zhou, Y. Wei, H. Liu, G. Zhang and X. Wu, *AAPS PharmSciTech*, 2010, **11**, 1350-1358.
3. L. Qiu, N. Jing and Y. Jin, *International journal of pharmaceutics*, 2008, **361**, 56-63.
4. N. Dos Santos, K. A. Cox, C. A. McKenzie, F. van Baarda, R. C. Gallagher, G. Karlsson, K. Edwards, L. D. Mayer, C. Allen and M. B. Bally, *Biochimica et biophysica acta*, 2004, **1661**, 47-60.
5. X. Mao, Y. Wo, R. He, Y. Qian, Y. Zhang and D. Cui, *Journal of nanoscience and nanotechnology*, 2010, **10**, 4178-4183.
6. E. Touitou, N. Dayan, L. Bergelson, B. Godin and M. Eliaz, *Journal of Controlled Release*, 2000, **65**, 403-418.